Available online at www.sciencedirect.com

ScienceDirect

Nuclear Physics B Proceedings Supplement 00 (2014) 1–4

Nuclear Physics B Proceedings Supplement

Thomas Schwindt - On behalf of the ATLAS Collaboration

Physikalisches Institut, Universität Bonn, Nussallee 12, D-53115 Bonn

Abstract

After the discovery of a Higgs boson at the LHC in $\gamma\gamma$, ZZ and WW final states in 2012, the ATLAS collaboration also observes an excess of data over the predicted background in $\tau\tau$ final states, which is consistent with the decay of the discovered Higgs boson with $m_H \approx 125$ GeV. With an observed (expected) significance of 4.1σ (3.2σ), this is evidence for the coupling of this Higgs boson to fermions. The multi-variate analysis of a dataset corresponding to 20.3 fb^{-1} of pp collisions at $\sqrt{s} = 8$ TeV is presented together with a separate cut-based analysis of the same dataset searching for $h/H/A \rightarrow \tau^+\tau^-$ decays in the context of the Minimal Supersymmetric Standard Model (MSSM). No excess of data over the expected backgrounds is observed in this search for additional Higgs bosons, and exclusion limits on the production cross section times branching fraction are derived and interpreted in the MSSM parameter space for different scenarios.

Keywords:

1. Introduction

With the discovery of a Higgs boson by the ATLAS [1] and CMS [2] collaborations, its predicted couplings to the gauge bosons of the electroweak interaction are confirmed. While the measured coupling strengths [3] only indirectly involve the fermions, a direct evidence for its coupling to fermions can be provided by the observation of Higgs boson decays to fermions. With a branching fraction of 6.3%, $H \rightarrow \tau\tau$ decays provide relatively clean final states in the pp collisions at the LHC, which can confirm the coupling of the Higgs boson to the heaviest lepton ($m_\tau \approx 1.78$ GeV). In the Minimal Supersymmetric Standard Model (MSSM), a second Higgs doublets is introduced. As a result, five Higgs bosons are predicted in total, of which the already discovered boson is a candidate either for the light (h) or the heavy (H) neutral and CP-even boson. In addition, a CP-odd neutral (A) and two charged ($H^\pm$) Higgs bosons are predicted. Depending on the mixing angle β between the two doublets, these particles obtain an enhanced coupling to τ leptons, so that $h/H/A \rightarrow \tau\tau$ decays provide a promising discovery potential for Supersymmetry.

2. Reconstruction of $\tau^+\tau^-$ Final States

Due to the short lifetime of the τ leptons, the $\tau\tau$ final states must be classified according to their sub-sequent decays. Each of the τ leptons can decay either into a lepton ($\tau^\pm_{\text{lep}} \rightarrow \ell^\pm \nu_\ell \nu_\tau$) or into hadrons ($\tau^\pm_{\text{had}} \rightarrow \tau^\pm_{\text{h}} \nu_\tau$). In ATLAS, the hadronic decays are reconstructed as τ_{h} objects, which are identified based on their shower shape in the calorimeter and their tracks in the inner detector. The distinction from other hadronic jets is based on Boosted Decision Trees (BDT), which keep the jet mis-identification rate below 1%. The abundance of jets in pp collisions, however, leads to significant background contributions especially for the hadronic decays. As a consequence, three different classes of final states (channels) $\tau_{\text{lep}}\tau_{\text{lep}}$, $\tau_{\text{lep}}\tau_{\text{had}}$ and $\tau_{\text{had}}\tau_{\text{had}}$ require separate analyses with different triggers and background compositions.

As a common contribution to all channels, $Z \rightarrow \tau\tau$ is a largely irreducible background and can mainly be distinguished via the invariant mass of the two τ leptons. The neutrinos cannot be detected directly, so that only the transverse component of their momentum sum can be observed as missing transverse energy E_T^{miss} in the detector. The reconstruction of the invariant mass from the visible decay products and $E_T^{\rm miss}$ is thus performed with the Missing Mass Calculator (MMC) [4], which uses a parametrisation of the τ lepton decay angles and obtains the most probable neutrino configuration from a kinematic scan.

3. Search for $H \rightarrow \tau\tau$ (Standard Model)

3.1. Analysis Strategy

The search for $H \rightarrow \tau\tau$ final states as predicted by the SM is performed in a multi-variate analysis, which relies on BDTs trained separately in two analysis categories for each of the three channels. The "VBF" category exploits the topology of forward jets produced in the vector boson fusion (VBF) process $qq\rightarrow qqH$ by selecting only events with two jets (anti-k_T, R=0.4) with a spatial separation of $\Delta\eta$>2.0-3.0 depending on the channel. The "Boosted" category gains an improved mass resolution by requiring a large transverse momentum (boost) of the reconstructed Higgs boson ($p_T(H)$>100 GeV), which is dominantly produced in the gluon fusion process $gg\rightarrow H$ together with one or more additional jets.

3.2. Event Selection

In the $\tau_{\rm lep}\tau_{\rm lep}$ channel, events are selected by single-lepton and di-lepton triggers. Exactly two leptons are required to be isolated and to have opposite charge, while events with an additional reconstructed $\tau_{\rm h}$-object are rejected. The dominant background from $Z\rightarrow\ell\ell$ is suppressed by selecting a window of the invariant mass of 30<$m_{\ell\ell}$<75 (100) GeV for same-flavour (different-flavour) lepton pairs in events with $E_T^{\rm miss}$>40 (20) GeV.

Events in the $\tau_{\rm lep}\tau_{\rm had}$ channel are selected by single lepton triggers, and exactly one reconstructed $\tau_{\rm h}$ object and one isolated lepton are required to have opposite charge. Backgrounds from Z+jets are suppressed by rejecting events with any additional lepton identified with reduced quality and isolation criteria. Events contributed by W+jets events, in which a jet is mis-identified as $\tau_{\rm h}$ object, are suppressed by requiring a low transverse mass of $m_T(\ell, E_T^{\rm miss})$<70 GeV. In both leptonic channels, events are rejected if any jet is identified by a b-tagging algorithm.

For the $\tau_{\rm had}\tau_{\rm had}$ channel, events with two $\tau_{\rm h}$ objects are selected with a di-$\tau_{\rm h}$ trigger. They are required to have opposite charge, while events with an additional lepton (e, μ) are rejected. In order to suppress the dominant multijet background with two mis-identified jets, $E_T^{\rm miss}$>20 GeV is required to be pointing between the $\tau_{\rm h}$ objects.

3.3. Background Estimation

The dominant $Z \rightarrow \tau\tau$ background is estimated from the data to avoid a potential mis-modelling of $E_T^{\rm miss}$ and additional jets in simulated events. A so-called embedding technique is thus applied to $Z \rightarrow \mu\mu$ events, in which the two muons in each event are replaced by decays of τ leptons. These are generated with corresponding kinematics including spin correlation effects implemented in TAUOLA [5, 6]. Other electroweak backgrounds such as Z+jets, W+jets and di-boson as well as top-quark production are estimated with simulated events, for which the normalisation is corrected to the data in corresponding control regions. Backgrounds with mis-identified leptons or $\tau_{\rm h}$ objects, however, are not reliably modelled by the simulation and must therefore be estimated with data-driven techniques.

For the $\tau_{\rm lep}\tau_{\rm lep}$ channel, templates for the multijet background are obtained from a control region with inverted lepton isolation criteria. Their normalisation is extracted from a fit to the distribution of the sub-leading lepton p_T in the data.

In $\tau_{\rm lep}\tau_{\rm had}$ final states, mis-identified $\tau_{\rm h}$ objects are contributed both from multijet and W+jets processes. The different mis-identification probabilities are measured in separate multijet and W+jets enriched control regions with inverted $\tau_{\rm h}$ identification criteria. These "fake-factors" are obtained as a function of p_T and the number of tracks associated to the $\tau_{\rm h}$ objects and are applied to extrapolate into the signal region.

The dominant background from multijet events in the $\tau_{\rm lep}\tau_{\rm had}$ channel is estimated by inverting the opposite charge requirement for the two $\tau_{\rm h}$ objects. For the resulting templates, the normalisation is obtained from a fit to the $\Delta\eta(\tau_{\rm h}, \tau_{\rm h})$ distribution in the data.

3.4. Boosted Decision Trees

On top of the basic event selection (Sec. 3.2), the separation of the $H \rightarrow \tau\tau$ signal from background is provided by BDTs, which are trained separately for the three channels and two categories. Each BDT is trained on a dedicated set of input observables, which all include the MMC mass (cf. Figure 1a). Additional observables are related to basic kinematics (e.g. $\sum |p_T|$) and the topology of $E_T^{\rm miss}$ exploited in m_T or an $E_T^{\rm miss}\phi$-centrality (cf. Figure 1b). For the VBF categories, the di-jet topology is exploited with several variables such as the spatial separation of the jets, their invariant mass $m(j, j)$ and the η-centrality of the visible τ decay products (cf. Figure 1c). In total, sets of 7-9 (6-9) observables are used for the training of BDTs in the VBF

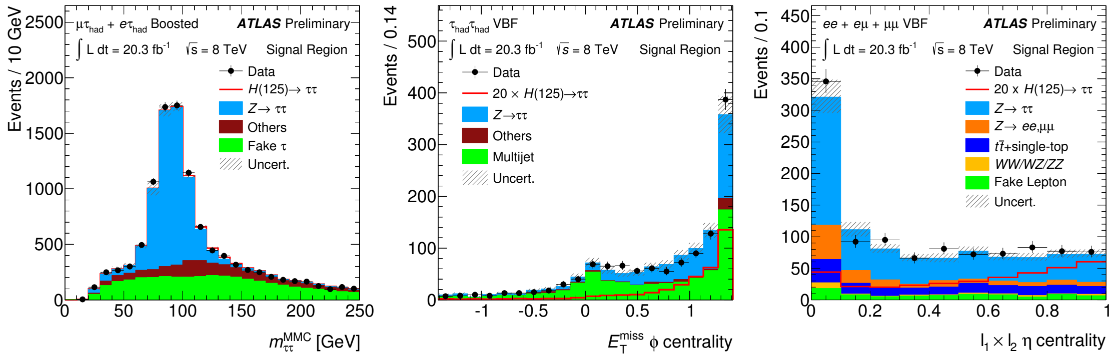

(a) (b) (c)

Figure 1: Input variables for the BDT training in the VBF category: (a) the MMC mass in $\tau_{\rm lep}\tau_{\rm had}$, (b) the $E_T^{\rm miss}\phi$-centrality in $\tau_{\rm had}\tau_{\rm had}$ and (c) the product of η-centralities of the leptons in $\tau_{\rm lep}\tau_{\rm lep}$ [7].

(Boosted) category. The correct modelling of the resulting BDT score distributions is validated in several control regions, which are enriched in the different background contributions from $Z \to \tau\tau$, W+jets, Z+jets and top-quark production.

3.5. Results

In a combined maximum likelihood fit to the data in all six BDT score distributions, estimators for the systematic uncertainties and certain normalisations of the background contributions are obtained together with the free floating signal strength parameter $\mu = \sigma_{\rm obs}/\sigma_{\rm SM}$. Figure 2 shows the background and signal composition in the relevant bins of all six BDT score distributions ordered by their S/B expectation. As a result of the fit, the observed signal strength for $H \to \tau\tau$ decays with m_H=125 GeV is determined to be:

$$\hat{\mu} = 1.43^{+0.31}_{-0.29}(\text{stat.})^{0.41}_{-0.30}(\text{syst.})$$

Within the asymptotic approximation [8], the significance of the observed excess over the background-only hypothesis is estimated to be 4.1σ. Although this exceeds the expected significance of 3.2σ, the result is found to be compatible with the signal+background hypothesis within 1σ and is thus evidence for the coupling of the Higgs boson to τ leptons. In order to visualise the compatibility of the result with the expected Higgs boson mass m_H=125 GeV, Figure 3 shows the MMC mass distribution, in which all events are weighted according to ln(1+S/B) of their corresponding BDT score bins.

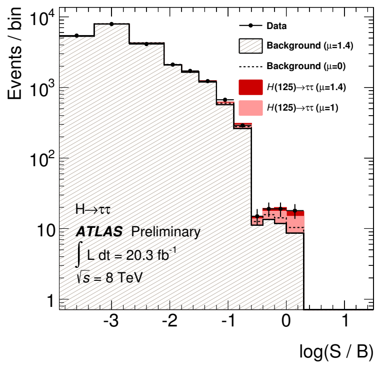

Figure 2: Combination of the BDT score bins from all categories and channels, ordered according to S/B [7].

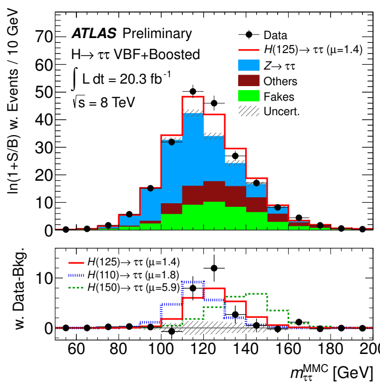

Figure 3: Distribution of the MMC mass combined for all categories and channels, weighted by ln(1+S/B) as described in the text [7].

4. Search for $h/H/A \to \tau\tau$ (MSSM)

4.1. Analysis Strategy

In contrast to the search for Standard Model $H \to \tau\tau$ decays with a fixed mass (m_H=125 GeV), the corresponding search for additional MSSM Higgs bosons must cover a wide mass range. It thus defines different signal regions with cut-based selections, which are optimised for a low-mass (90<m_A<200 GeV) and a high-mass regime (m_A>200 GeV). Similar to the τ leptons, also the coupling of the MSSM Higgs bosons to b-quarks is enhanced. Dedicated signal regions select final states with b-tagged jets targeting the Higgs boson production in association with b-quarks.

4.2. Categorisation

With a similar basic selection as described in Section 3.2, the $\tau_{\rm lep}\tau_{\rm lep}$ channel only includes $e\mu$ final states. A b-tag and a b-veto category are defined depending on the presence of a b-tagged jet in the event.

Similarly, a b-tag (b-veto) category is defined in the $\tau_{\rm lep}\tau_{\rm had}$ channel, in which the W+jets background is suppressed with m_T<60 (45) GeV. An additional high-mass category is included, in which the difference $p_T(\tau_{\rm h}) - p_T(\ell)$>45 GeV is exploited instead of m_T.

For the $\tau_{\rm had}\tau_{\rm had}$ channel, an additional category is included, for which events with $p_T(\tau_{\rm h})$>150 GeV are selected by a single-$\tau_{\rm h}$ trigger. While this selection targets signal events with a high-mass, the di-$\tau_{\rm h}$-triggered events enter the low-mass category without further selection on b-tagged jets.

4.3. Background Estimation

The $Z \to \tau\tau$ background is estimated with the embedding method as described in Section 3.3, and other electroweak and top-quark backgrounds are obtained from simulation. Templates for the multijet backgrounds in all channels are extracted from control regions with inverted charge requirement. The normalisation in the signal region is provided by extrapolation factors, which are obtained from similar opposite- and same-charge control regions with inverted lepton isolation or $E_T^{\rm miss}$ requirement ($\tau_{\rm had}\tau_{\rm had}$).

4.4. Results

No excess of data over the expected background is observed in the seven signal regions. Exclusion limits are therefore derived on the production cross section of additional Higgs bosons predicted in the MSSM, which can be translated to exclusion limits on parameters of the MSSM. Its Higgs sector can be described by m_A and $\tan\beta$, while the dependence on further parameters is fixed by choosing a specific benchmark scenario. As an example, Figure 4 shows the excluded range of $\tan\beta$ as a function of m_A for the $m_h^{\rm max}$ scenario, in which m_h is maximised for a given $M_{\rm SUSY}$=1 TeV. The lowest constraint in this scenario can thus exclude $\tan\beta$ > 5.4 for m_A=140 GeV.

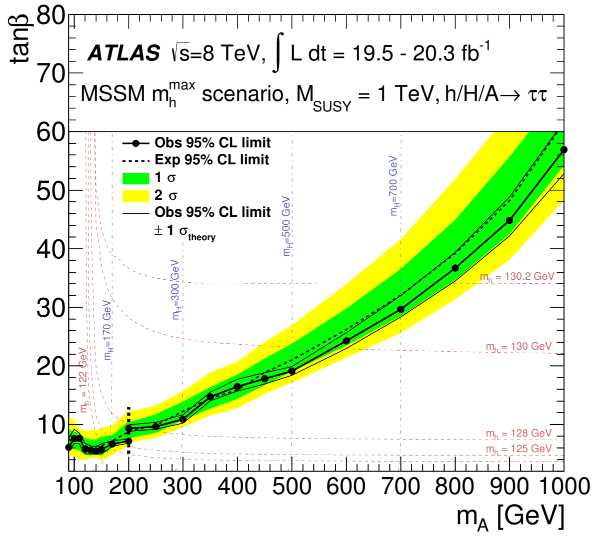

Figure 4: Exclusion limits from the MSSM $H \to \tau\tau$ analysis in the $m_h^{\rm max}$ scenario [9].

References

[1] ATLAS Collaboration, 2008 JINST 3 S0800.
[2] CMS Collaboration, 2008 JINST 3 S0800.
[3] ATLAS Collaboration, Phys. Lett. B 726 (2013) 88-11.
[4] A. Elagin et al., NIM A 654 (2011) 481-489.
[5] S. Jadach et al., Comp. Phys. Comm. 76 (1993) 361-380.
[6] Z. Czyczula et al., Eur.Phys.J. C72 (2012) 1988
[7] ATLAS Collaboration, ATLAS-CONF-2013-108, http://cdsweb.cern.ch/record/163219.
[8] G. Cowan et al., Eur. Phys. J. C 71 (2011) 155.
[9] ATLAS Collaboration, arXiv:1409:6064, submitted to JHEP.